

Article

Enhanced Photocatalytic Activity of C-doped TiO₂ under Visible Light Irradiation: A Comparison of Corn Starch, Honey, and Polyethylene Glycol as a Carbon Sources

Sittipong Au–pree¹, Phiphop Narakaew², Siwat Thungprasert¹,
Theeraporn Promanan¹, Aphiruk Chaisena¹, and Samroeng Narakaew^{1,*}

¹ Department of Chemistry and Applied Chemistry, Center of Excellence for Innovation in Chemistry, Faculty of Science, Lampang Rajabhat University, Lampang 52100, Thailand

² Department of Physics, Faculty of Science, Lampang Rajabhat University, Lampang 52100, Thailand

*E–mail: krachodnok@lpru.ac.th (Corresponding author)

Abstract. Titanium dioxide (TiO₂) represents an effective photocatalyst for removal of polluted water; however, it has a limitation of active under small part of ultraviolet light region from sun spectrum. Herein, reported the carbon doping TiO₂ (C-doped TiO₂) by using various carbon sources such as corn starch, honey, and polyethylene glycol, for improving the electronic and photocatalytic properties of TiO₂. The responded visible light photocatalysis was synthesized via the ultrasonic–assisted sol–gel method and characterized by X-ray diffraction (XRD), fourier transform infrared (FT–IR) and X-ray photoelectron (XPS) spectroscopy, field emission scanning electron microscopy (FE–SEM), energy dispersive X-ray spectroscopy (EDS), and UV–vis spectroscopy. The results showed that the photocatalytic C-doped anatase TiO₂ nanoparticles have the narrowest band gap down to 2.71 eV with increase the carbon doping up to 2.0% by weight from corn starch as external carbon source. XPS result reveals carbon substitution of titanium positions in the anatase TiO₂ structure and also to precipitate at the surface of TiO₂. As compared photodegradation efficiency under ultraviolet light, observed 87 %MB maximum photoremoval in neutral aqueous solution within 1 hour reaction time under visible light irradiation. While doping with other carbon sources, C-doped anatase TiO₂ showed low photocatalytic activity. Hence, great strategy of wastewater treatment application in large scale pilot plant, selected low cost of corn starch acted as an external carbon source for promoted an excellent visible light nano-anatase TiO₂ photocatalytic immobilization on the modified glass supporter throughout adhesive waterproof glue.

Keywords: C-doped anatase TiO₂ nanoparticles, methylene blue degradation under visible light region, ultrasonic–assisted sol–gel method, corn starch, honey, PEG1500.

ENGINEERING JOURNAL Volume 25 Issue 1

Received 14 April 2020

Accepted 29 December 2020

Published 31 January 2021

Online at <https://engj.org/>

DOI:10.4186/ej.2021.25.1.53

1. Introduction

Titanium dioxide (TiO₂) has been employed as the photocatalyst for a several decades [1] with their excellent properties as follows; stable material, non-toxicity [2], narrow band gap energy, environmentally friendly [3], good chemicals, physicals, optical and electrical properties [1, 4].

Miranda-García et al. (2010) [5], used immobilized TiO₂ to purify of polluted water by advance oxidation processes (AOPs) in the results, showed the high performance for degraded all of the organic pollutants under the light illuminance absorbed under ultraviolet (UV) light irradiation. It can be explained by their morphological structure of TiO₂ which has main crystal polymorphs such as tetragonal anatase and rutile structures, which contains four and two TiO₂ units per unit cells, respectively, and other, the brookite turning to orthorhombic structure with eight TiO₂ units per unit cell [6]. The atomic alignment in the difference structure has an effectively for charge carrier in electronic properties as well as the band gap energy (E_g) that were reported as 3.05, 2.98 and 3.20 eV in the anatase, rutile, and brookite crystalline phase respectively [7]. Accordingly, the verities for improvement of photocatalytic activity in TiO₂ were assembled by many strategies for adjusted and modified the physical and chemical properties such as increasing the surface area, reducing the particle sizes, mixing double-phase structure, moreover, reducing the band gap energy for extended to visible light absorbed by doping with metals or non-metals into TiO₂ structure [8, 9]. Hence, the recent researches having focus on reducing the band gap of TiO₂ by a several incorporated with materials doping as follows; metal dopants (Cu, Zn, Fe, Cr, Nb, W, Ag, Co, Ta, Mo, Mn, Ni, V, Au, Pd, Pt, Rh or Ru) [10–33, 48], including non-metal dopants (C, B, S, N, F and Cl) [34–63] to enhance the electronic properties of TiO₂ for active at the visible (Vis) light region. Normally, the sunlight has more Vis-light (40%) as compared to UV light (5%). The advantages of metal dopants are showed the narrow band gap energy [64], thus, effected to visible light absorbed, but, the disadvantages of metal dopants will be toxicity in the aquatic environment [65]. Moreover, the metals can be reduced the photocatalytic efficiency by the metal cation vacancies, that can act as electron trap sites which more positive sites can induce electron recombination [48]. While non-metal doping has been more efficient for photocatalytic activity by an anion vacancies can trap photogenerated electrons in the conduction band and protecting the electron (e⁻) – hole (h⁺) recombination [3, 66].

From those non-metals doping, carbon was applied to doping into TiO₂ structure which were reported by several published articles in the past decade. The several carbon sources containing of the internal titanium precursor; titanium carbide (TiC) or titanium butoxide (TBO) [51–52], or adding external carbon sources; tween 80 [39], tetrabutylammonium hydroxide (TBAOH) [52],

alkylammonium, urea, and ethanol [53], activated carbon (AC) [54–55], sucrose [56], melamine borate [57], carbon nanotube (CNTs) [58], glucose [59], graphite [60], and ethylene chlorotrifluoroethylene (ECTFE) [61] and polyethylene glycol (molecular weight of 6000 g/mol, PEG6000) [62] were used. The carbon doped TiO₂ promoted the narrowing band gap energy with the high efficiency for organic pollutant removal under Vis-light region with carbon doping offer unique advantages such as chemical inertness, stability and tuneable structural and electrical properties [63].

Along with these backgrounds, the aim of this research focuses on improving the electronic and photocatalytic properties of TiO₂ apply for purification of polluted water under Vis-light region by doping with difference carbon sources such as natural corn starch powder and liquid honey which are non-toxicity, low cost to prepare, and a raw material, and other synthetic carbon doping source such of polyethylene glycol (molecular weight of 1500 g/mol, PEG1500) which these carbon doping sources are unreported yet from literature reviews.

2. Experimental Section

2.1. Materials

The TiO₂ precursor was prepared from titanium tetraisopropoxide (TTIP) was ordered from Sigma-Adrich, Co. Ltd. Glacial acetic acid solution (HOAc) was derived from Flinn Scientific Ltd. 95%v/v. Ethanol (EtOH) was purchased from RCI Lab Scan Ltd. Methylene blue (MB) was obtained from Gammaco (Thailand) Co. Ltd. Polyethylene glycol (PEG1500) with Mw. 1500 g mol⁻¹ was acquired from Loba Chemie PTV. Ltd. 15%v/v hydrofluoric acid (HF) was ordered from the Thai commercial shop. Commercial corn starch and liquid honey were obtained from Continental Food Co., Ltd. and Pattaratumrong Co., Ltd, respectively. Deionized water was used in the all experiments, and all chemical reagents were used without any purification.

2.2. Synthesis of Photocatalytic C-doped TiO₂

TiO₂ and C-doped TiO₂ nanoparticles were synthesized by an ultrasonic assisted sol-gel method as reported in [67], mixed 100 mL EtOH and 0.2 mL HOAc in the beaker and stirred for 5 minutes, after that, dropped 9 mL TTIP continuously. Next, doped carbon from difference sources; corn starch (sample code: xC-TiO₂), honey (sample code: xH-TiO₂), and PEG1500 (sample code: xP-TiO₂) with x = 0.5, 1.0, and 2.0%wt. Then, the mixed solutions were sonicated under ultrasonic irradiation (40 kHz, 150 W, Elmasonic P 30 H) for an hour. Thus, allowed transform TiO₂ to sol-form and then brought to centrifuged machine (Universal 32, Hettich 1605) to separate the particles under 3000 rpm for 10 minutes. Then, dried at 105°C for overnight (12 hours) after that calcined at 400°C for 2 hours under N₂

atmosphere to transformation amorphous TiO₂ and C-doped TiO₂ to completely formed nano-crystalline of white powder of TiO₂, and white to brawn to grey, brawn to grey to black, and white to brawn C-doped TiO₂ powders relation with increasing the 0.5 to 2.0%wt. of corn starch, honey, and PEG1500.

2.3. Characterization

Some physicochemical properties of carbon sources doping were characterized including colour, pH value by using pH meter (Eutech instruments pH 700), and density value by using digital refractometer (Atago, Japan) moisture content (MC), fixed carbon (FC), volatile matter (VM) and ash by proximate analysis. Chemical compositions of dried carbon materials were performed by CHNS/O analyzer (Thermo Scientific TM FLASH 2000).

Phase characterization and crystallographic structure of the synthesized C-doped TiO₂ samples were carried out from powder X-ray diffraction (XRD), Rigaku MiniFlex 600, with X-ray sources from Cu K_α irradiation ($\lambda = 1.5406 \text{ \AA}$) and operated at 40 kV, 15 mA, 2 θ range scan of 20–80°, step scanned of 0.02°, speed scanned of 20°/minutes. After that, phase identification was done by comparing with the diffraction patterns (JCPDS card) data base by X' Pert High Score software and collection of simulated XRD powder patterns.

The surface chemistry of samples was investigated by X-ray photoelectron spectrometry (XPS), Axis Ultra DLD, Kratos Analytical Ltd. The sample introduction chamber is usually pumped by turbomolecular pumps capable of attaining vacuum levels of $\sim 5 \times 10^{-8}$ Pa (or $\sim 5 \times 10^{-10}$ mbar) with Mg K_α or Al KCY radiation in X-ray photoelectron spectrometer (XPS), Axis Ultra DLD, Kratos Analytical Ltd.

The functional groups of the carbon doping sources and the synthesized C-doped TiO₂ photocatalytic samples were characterized by fourier transform infrared spectroscopy (FT-IR), Shimadzu (FTIR-8900). The samples were prepared by potassium bromide (KBr) pellets method and scanned range around 4000–400 cm⁻¹.

The band gap energy (E_g) of the synthesized C-doped TiO₂ samples were analysed by UV-Vis diffuse reflectance electronic spectra by using UV-Vis spectrophotometer (Shimadzu UV-3600 Plus). The performed at wavelength of 800–200 nm. After that, the UV-Vis spectra were undertaken by "Tauc Plot" technique. The Tauc plot were showed the quantity $h\nu$ (the energy of the light) on the abscissa and the quantity $(\alpha h\nu)^{1/r}$ on the ordinate, where α is the absorption coefficient of the material. The value of the exponent $r = 2$ denotes as indirect optical transition mode [68-69]. Thus, discuss the intersection of linear by drawing a tangent line of the curve until intersection with X-axis.

The morphology of the all products were analysed by field emission scanning electron microscope (FE-SEM), JSM 6335 F, operating at 15.0 kV as accelerating voltage.

The samples were dispersion in 5.0 mL EtOH by sonication and dropped on copper tape. Then, stick on SEM specimen stubs and coated with Gold (Au) by ion plasma coating technique for 10 mins. Then put in SEM analysis machine that was equipped with electron dispersive X-ray spectrometer (EDS) for discriminating the percentages of the elements in the sample C-doped TiO₂ and titanium (Ti), carbon (C) and oxygen (O) elemental distribution mapping. Thus, it was used Image J software for helped to determine the particles sized in SEM micrograph.

2.4. Photocatalytic Activity

For the employing C-doped TiO₂ photocatalytic samples with easy to regenerate after completed degradation of MB as dyed organic model. The powder of synthesized photocatalytic samples were immobilized on the modified glass slide by using commercial adhesive waterproof glue. Prior, the modified glass slide (25 × 75 × 1 mm, width × length × thickness) which was etched at one side by using 15%v/v. HF for 60 mins into 24 circle concaves (each 5.5 mm diameter with 0.25 mm etching-depth) fine patterned glass panel surfaces with surface area of 4,332 mm². Those modified glasses were cleaned with deionized water and dried in ambient temperature. After that, 20 mg C-doped TiO₂ in the mixed solution of 9.8 mL EtOH and 0.2 mL HOAc and continuously stirred for 10 mins to form the colloid of C-doped TiO₂ samples and each one was put into the spray bottle. Then, spray bottle was located at 5 cm height on the modified glass supporter covered with adhesive waterproof glue. 10 mL C-doped TiO₂ colloid was sprayed on its surface and dried at 80 °C for 30 mins for alcohol removal. The images of the surface of TiO₂ and nine types of C-doped TiO₂ films are shown in Fig. 1.

In the photodegradation process were operated in open system. The processing was used 200 mL of 6.25 × 10⁻⁶ M MB in the aqueous solution and controlled the pH = 7 by HOAc. Then, the photooxidation were studies under UV-light irradiation (UV lamp TL 20W/05, Philips (Thailand) Ltd.) with wavelength at 350 nm and under Vis-light irradiation (the fluorescent lamp from Philips (Thailand Ltd.)). The 10 mL of the sample solution were collected, centrifuged, and monitored by using UV-visible spectrophotometer (Agilent Cary-60) in absorption mode and operated wavelength at 664 nm in every 10 mins until an hour. Quart cuvette was used in this process. The performance of photocatalytic activity were calculated by using equation (Eq. (1)) as shown below

$$\% \text{MB degradation} = \frac{C_0 - C}{C_0} \times 100 \quad (1)$$

where C_0 is the initial concentration of MB solution and C is the final concentration of MB solution after degradation time.

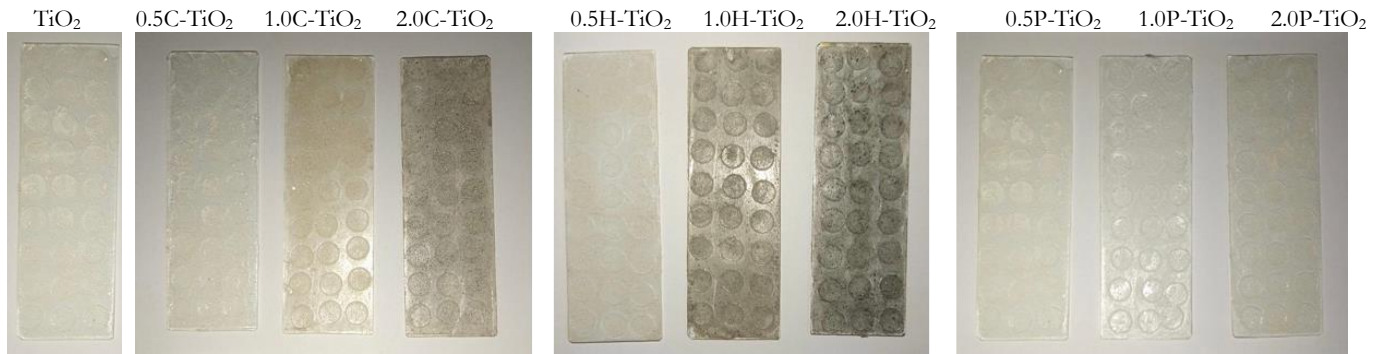


Fig. 1. The optical images of the surfaces of TiO_2 and nine types of C-doped TiO_2 films.

3. Results and Discussion

3.1. Characterization of the Carbon Doping Sources

Table 1 shows the some physicochemical properties of the carbon dopant sources. Different carbon dopant sources have different colour appearance. pH value of honey and PEG1500 are in weak acid while corn starch is neutral. The state of the carbon dopant sources are observed in different, corn starch and PEG1500 are similar state, except honey in liquid form. Therefore, moisture content of honey is higher than natural corn starch and synthetic PEG1500. While synthetic PEG1500 has higher volatile matter. Moreover, observed the carbon composition of dried powdered corn starch,

honey and PEG1500 are 13.25, 13.22 and 17.99 % db. Figure 2. shows FT-IR spectra of those three organic carbon doping sources. The broad band in the range of $3,125\text{--}3,516\text{ cm}^{-1}$ is identified to the water in liquid honey. Also, observed the peaks at $2905\text{--}2,929$ and $1,023\text{--}1,156\text{ cm}^{-1}$ were corresponding to C–H, and C–O and C–O–C stretching. The peaks in the range of $1,603\text{--}1,645$, $1,446\text{--}1,457$ and $758\text{--}953\text{ cm}^{-1}$ were assigned to O–H bending, CH_2 symmetric scissoring and C–O–C ring vibrations, respectively as reported in [70]. The mean small peaks at about $2,356\text{--}2,364\text{ cm}^{-1}$ contributed the carbon dioxide (CO_2) asymmetric stretching vibration from atmosphere.

Table 1. The some physicochemical properties of the carbon doping sources.

Content	Corn starch	Honey	PEG1500 ^a
pH	7.32	5.21	6–7
	at 29°C	at 29°C	at 23°C
Colour and state	milky white solid power	golden yellow liquid	clear colourless solid power
Density (g/cm^3) at 20°C	1.3092	1.3812	1.1250
MC (%)	7.60 ± 0.04	17.92 ± 0.20	0.00
FC (%)	1.47 ± 0.20	0.03 ± 0.02	0.22 ± 0.15
VM (%)	90.91 ± 0.21	82.03 ± 0.20	99.77 ± 0.14
Ash (%)	0.02 ± 0.01	0.02 ± 0.01	0.00
C (% db.)	13.25	13.22	17.99
H (% db.)	19.66	20.29	27.53
O (% db.) ^b	67.07	66.47	54.48

^a MSDS data from Loba Chemie Laboratory Reagents & Fine Chemicals

^b O element was balanced = $100 - \text{C} - \text{H} - \text{Ash}$

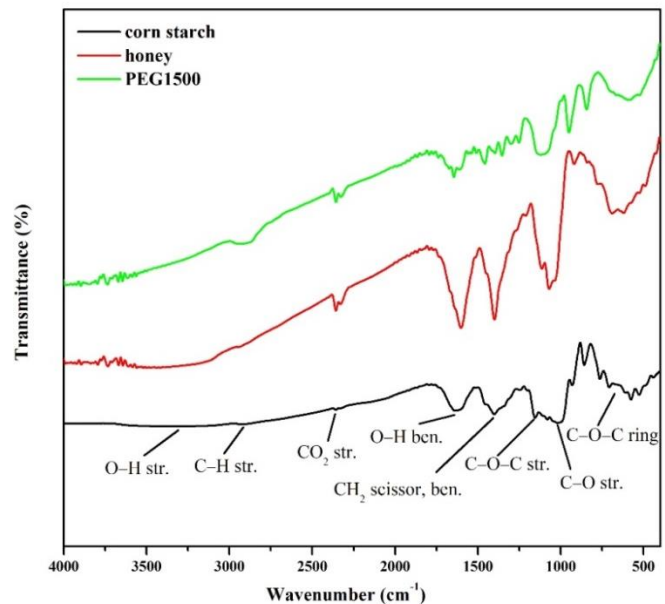


Fig. 2. FT-IR spectra of carbon doping sources.

3.2. Characterization of the Synthesized C-doped TiO₂

Phase characterization and crystallographic structure of all synthesized C-doped TiO₂ were investigated by XRD (Fig. 3). The main diffraction peaks were observed at 2θ about 25.30°, 37.93°, 48.00°, 53.98°, 54.98°, 62.74°, 68.93°, 69.76° and 75.26° consistent to (101), (004), (200), (105), (204), (220) and (215) planes of pure anatase TiO₂. The X' Pert High Score software was employed to determine the TiO₂ structure. Its structure was confirmed by JCPDS card no. 01-073-1764, that all synthesized C-doped TiO₂ crystallized in tetragonal structure with space group I₄₁/amd. In addition, it could be assumed when using carbon doped into the TiO₂ structure, the dopant did not an affected to TiO₂ morphological structure as agreement with other studies

[74]. The mean sizes of the synthesized C-doped TiO₂ nanocrystals were calculated by Debye-Scherrer's equation as (Eq. (2))

$$D_{hkl} = \frac{K\lambda}{\beta_{hkl} \cos\theta} \quad (2)$$

where λ is the wavelength of incident X-rays for Cu K_α (λ = 1.5406 Å), β_{hkl} is the full width at half maximum (FWHM) of the anatase TiO₂ peak at (101) plane (in radians), θ corresponding the TiO₂ peak at 2θ = 25.30°, and K is a constant, which has been assumed to be 0.9, in this results were corresponding to the previously studies [71-73].

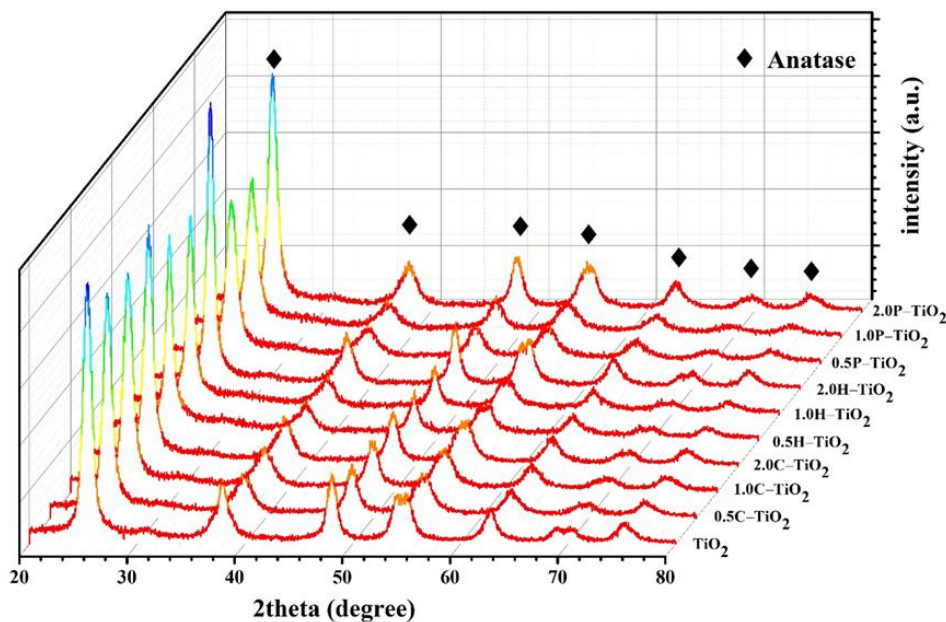


Fig. 3. The XRD patterns of TiO₂ and the as-synthesized C-doped anatase TiO₂.

Table 2. The particles sizes, band gap energy and elemental composition of anatase TiO₂ and the as-synthesized C-doped anatase TiO₂.

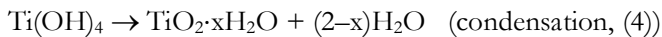
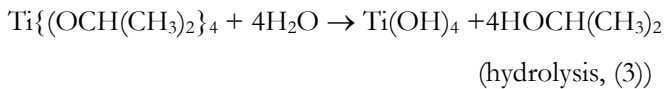
Conditions	FWHM ^a (β, °)	Particle size ^a (nm)	E _g ^b (nm, eV)	Elemental composition ^c (%wt.)			
				%Ti	%O	%C	%C ^d
TiO ₂	0.8722	9.14	401, 3.09	61.31	36.03	2.66	18.06
0.5C-TiO ₂	0.9518	8.55	409, 3.03	61.08	33.43	5.49	
1.0C-TiO ₂	1.1255	7.23	434, 2.86	34.46	56.60	8.94	
2.0C-TiO ₂	1.1005	7.40	458, 2.71	43.09	44.94	11.98	19.69
0.5H-TiO ₂	0.7829	10.40	400, 3.10	56.70	39.20	4.10	
1.0H-TiO ₂	0.7831	10.40	428, 2.90	54.82	40.70	4.48	
2.0H-TiO ₂	0.7341	11.09	448, 2.77	55.70	39.31	4.99	
0.5P-TiO ₂	0.9346	8.71	408, 3.04	59.84	36.95	3.21	
1.0P-TiO ₂	1.0026	8.12	414, 3.00	56.09	40.48	3.44	
2.0P-TiO ₂	0.9707	8.39	418, 2.97	59.67	36.55	3.78	

^a From XRD patterns and calculated by Debye-Scherrer's equation

^b From Diffuse reflectance spectra and calculated by Tauc plot technique

^c From EDS spectra and ^d the selected some XPS spectra

Which the particle sizes of all crystalline products showed the range about ~7-11 nm as shown in Table 2. In usually, the sol-gel process for nano-catalyst, it was having an important reaction in the sol-gel process: hydrolysis and condensation. The reaction rate depends on pH, the ratio of water to metal and temperature, therefore controlling these factors in different conditions thus causing sol and gels with different properties and structures. The reaction was written as follows.



XRD results with Debye-Scherrer's equation observed the different carbon sources led to different crystallite size of the as-synthesized C-doped TiO₂ products as follow of H-TiO₂>P-TiO₂>C-TiO₂. The size of H-TiO₂ nanoparticles are higher than other carbon doping sources because of honey has normally liquid state which

consists of 17.92 %MC, while other are in dried powder of PEG1500 and 7.6%MC for corn starch as reported in Table 1. shows the hydrolysis and condensation mechanism of TTIP to TiO₂ or the as-synthesized C-doped TiO₂ using the ultrasonic assisted sol-gel method. The water was obtained from not only honey in liquid form but also 95% ethanol (5% water) and moisture in air that can be reacted faster with TTIP to give Ti(OH)₄ sol precursor and then polycondensation occurred immediately, milky colloid solution, resulting to quick agglomeration with bigger particles size of TiO₂ than other carbon doping source, although, using the ethanol solvent prevented by hydrogen bonded to O-bridging of Ti-O-Ti structure at pH = 3 (HOAc) as reported in [77] or more acidity of honey as shown in Fig. 4. Moreover, observed the crystallite size of as-synthesized C-doped TiO₂ decreased when using the amount of carbon sources of 1%wt. doping or higher, except using honey as carbon source.

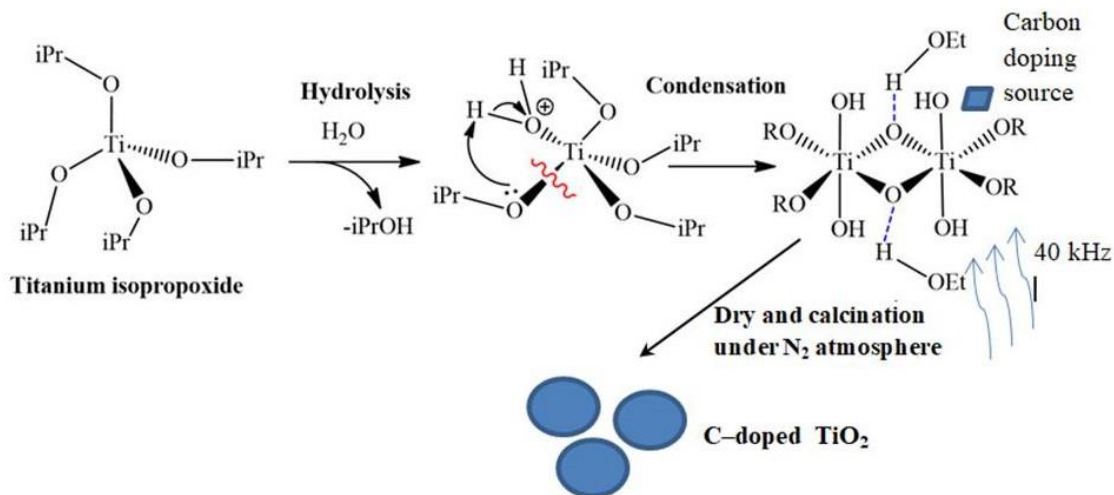


Fig. 4. The schematic synthesis of C-doped TiO₂ by using ultrasonic assisted sol-gel method.

The XPS technique can confirm the chemical surface of C-doped TiO₂ samples. The XPS survey spectra of TiO₂ and the as-synthesized C-doped TiO₂ samples in different external carbon sources doping were shown in Fig. 5a. From the XPS results that clearly confirmed the carbon doping into the anatase TiO₂ structure with either internal or external carbon sources. Obviously, both of them had contained Ti, O and C elements which characteristic peaks of binding energies at about 458.10 eV (Ti 2p), 530.10 eV (O 1s) and 285.10 eV (C 1s) atomic composition of 20.02, 48.24 and 31.75%atom or 18.06%wt. respectively, for TiO₂ with carbon self-doping. In this case, the carbon self-doping is from the same starting material of TiO₂, the TTIP consisting of four isopropoxide ligands. The other hand, the atomic composition of Ti, O and C elements in the selected C-doped TiO₂ (2.0C-TiO₂) was 19.46, 46.38 and 34.16 % atom or 19.69%wt. respectively, which was confirmed that the amount of carbon atom increase about 2.41%atom or 1.63%wt. as compared with the carbon

self-doped TiO₂. The C-doped TiO₂ (2.0C-TiO₂) lattice verification was confirmed by high-resolution XPS technique. The C 1s XPS spectra consisting four different environments with binding energies observed in the region of 298 eV to 270 eV as seen in Fig. 5b, the peaks appeared at 284.5 eV was attributed to external hydrocarbon contamination on the photocatalytic surface or the hybridization of carbon species (C-C) [78] and other three peaks at 285.14, 286.42 and 288.74 eV were characteristic of the oxygen bond species C-O, C=O and O-C=O respectively, the above results are also supported by FT-IR spectra as shown in Fig. 6 which was appeared at 1,074.76 cm⁻¹. Thus, demonstrated to C was incorporated into TiO₂ lattice by substituted Ti atomic position and existed in the form of CO₃²⁻ [79-81], that can be confirmed with by determination of Ti 2p high-resolution XPS spectra in Fig. 5c. Normally, Ti 2p core levels have appeared two main peaks of binding energies at 458.8 eV (Ti 2p_{3/2}) and 464.5 eV (Ti 2p_{1/2})

with different binding energies value of ~ 5.7 eV. There is in good agreement that no type of Ti-C bond formation or no carbon substituted at the oxygen atomic position.

The occurrence of O1s high-resolution presented in the XPS spectra shown in Fig. 5d were provided the

cooperated of O atom with C and Ti atoms. The four peaks different environments appeared at about 530.10, 531.26, 532.08 and 533.19 eV that can be assigned to Ti-O-Ti, C=O and COO, Ti-OH, and C-OH and C-O-C.

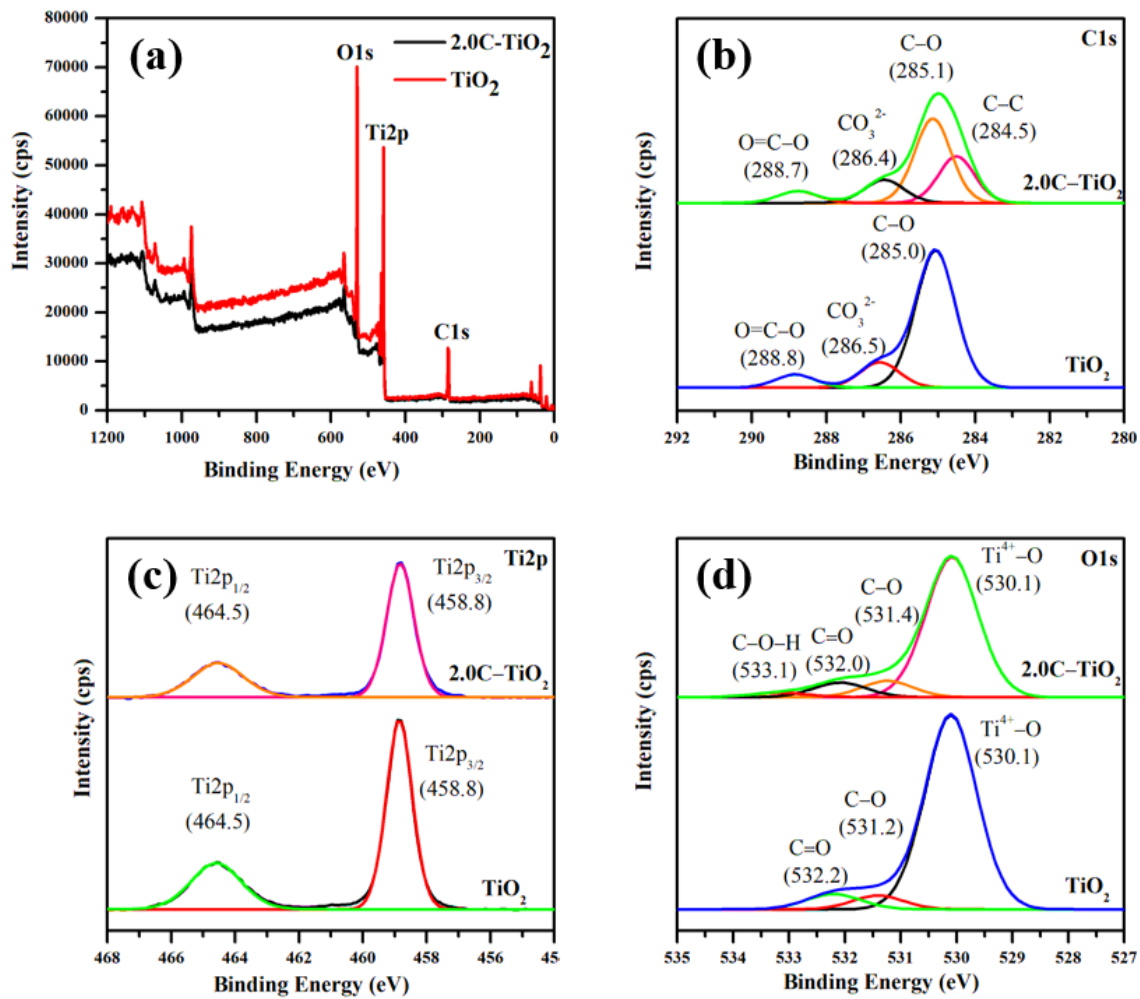


Fig. 5. XPS spectra of TiO_2 and the selected as-synthesized C-doped TiO_2 (2.0C- TiO_2) in (a) survey mode, (b) high-resolution XPS spectra of C 1s, (c) Ti 2p, and (d) O 1s.

Moreover, the functional groups of the as-synthesized C-doped TiO_2 were confirmed by FT-IR technique, in FT-IR spectra (Fig. 6) showed the broad band in the range of $3,100\text{--}3,400\text{ cm}^{-1}$ and the peak at $1,615.65\text{ cm}^{-1}$ were corresponding to O-H stretching and bending vibration, cause O-H group from the water in the air that can be adsorbed by TiO_2 surface. The mean small band at about $2,343.24\text{ cm}^{-1}$ contributed CO_2 asymmetric stretching vibration from atmosphere. Next, a weak peak was observed at $1,400.00\text{ cm}^{-1}$ caused by Ti-OH stretching vibration and the two signals that was observed at $1,124.52\text{ cm}^{-1}$ and $1,067.75\text{ cm}^{-1}$ demonstrated to the stretching and bending vibration of Ti-O-C cause by carbon substituted to titanium atom thus corresponding to [82]. The peak in 669.98 cm^{-1} was also detected clarify to the Ti-O bending vibration. All the results in this case were corresponding to previously reported [17, 18, 67].

Diffuse reflectance spectra of C-doped anatase TiO_2 as Fig. 7a and Tauc plot spectra showing the relationship between the absorbance value and the wavelength, it can analyse the band gap energy by Plunk's law (reversed the wavelength to energy value) were shown in Fig. 7b-d. The band gap energy can be calculated from the extrapolation of the absorption edge onto the energy axis, E_g , of C-doped anatase TiO_2 from different carbon sources as shown in Table 2. Especially, estimated band gap energy reduced form 3.09 (TiO_2) to 2.71 eV or 458 nm when using corn starch as carbon doping as found in other carbon sources [39, 53-62]. All products have band gap energy move to red shift of Vis-light adsorption with increase the amount of carbon doping as similar trend observed by using PEG6000 as carbon source in [65].

From SEM images are illustrated in Fig. 8-9, represented the morphologies of TiO_2 and the as-synthesized C-doped anatase TiO_2 with observed the

small particle seems like a spherical shape and forming to cluster with some agglomeration during annealed processes as reported in [67] and can be roughly measured particle sizes assisted by Image J software. At the results, the nanoparticle sizes were measured in an average range of 7–11 nm which corresponding particles sizes were calculated by Debye–Scherrer's equation as (Eq. (2)) from XRD results (Table 2). Especially, the

catalyst particles are bigger when using honey as carbon source due to higher water content. In Fig. 10 represents EDS mapping of 2.0C-doped anatase TiO₂, the elementals amount of synthesized C-doped TiO₂ including to the distribution of Ti (Fig. 10b), C (Fig. 10c) and O (Fig. 10d) elements, and (e) EDS spectrum respectively.

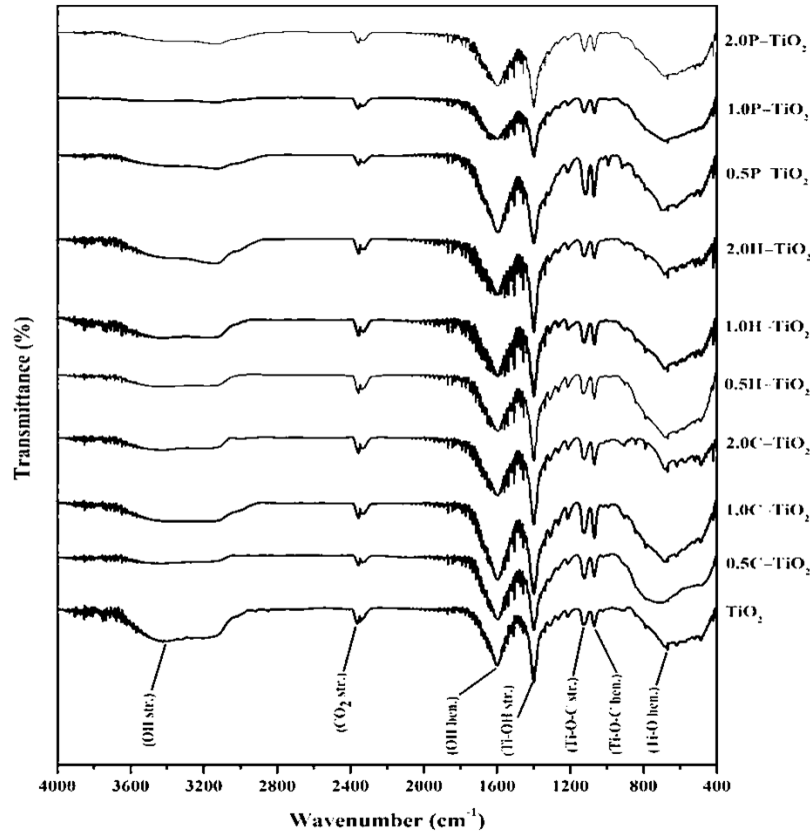


Fig. 6. FT-IR spectra of TiO₂ and the as-synthesized C-doped TiO₂.

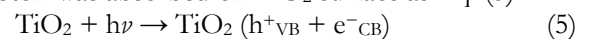
3.3. Photocatalytic Activity

In Fig. 11b shows the cross-section SEM image of the selected as-synthesized 2.0C-TiO₂ particle on the modified glass slide covered with waterproof glue layer of ~ 52 nm as compared with only a bare textured glass (Fig. 11a). The top-view optical images of the as-synthesized C-doped TiO₂ films show the uniform particle distribution on the surfaces by spraying method as shown in (Fig. 1 and 11b).

From MB removal results, C doping with 2.0wt% from corn starch, honey, and PEG1500 into TiO₂ structure that can be significantly enhanced its TiO₂ photocatalytic activity of ~87, ~61, and ~51 %MB degradation under Vis-light irradiation while observed ~33, ~35, and ~35% MB degradation under UV light irradiation with reaction time of 1 hr as compared to 44 and 20% MB degradation of TiO₂ as shown in Fig. 12. Due to not only the suitable 7–11 nm anatase C-TiO₂ nanoparticles are active under the light Vis-light irradiation between 400–458 nm. But also, the more surface area of the modified glass supporter which could

be assisted to improve the light absorption surface and the properties of indirect band gap energy in anatase TiO₂, in addition to, can be reduced the rate of surface recombination with electron in the MB degradation process as found in [12]. It showed significantly the excellent performed Vis-light photocatalysis as compare to TiO₂ which was found C-self doping character. The impact of this cause, can be discussed with the increasing of performance in MB degraded under Vis-light process (Fig. 12b) that showed the more efficient MB degraded than the UV process (Fig. 12a) in 1 hour reaction time. Moreover, in this study, was founded the carbon dopant from corn starch can be enhancing the photochemical properties of TiO₂ for higher %MB degraded than either two carbon doping sources.

The MB degradation mechanism can be described in Eq. (5)–(6) and Fig. 13 the first step of degradation reaction, the photo-excited electrons at conduction band and positive holes at valence band were generated when the photon was absorbed on TiO₂ surface as Eq. (5):



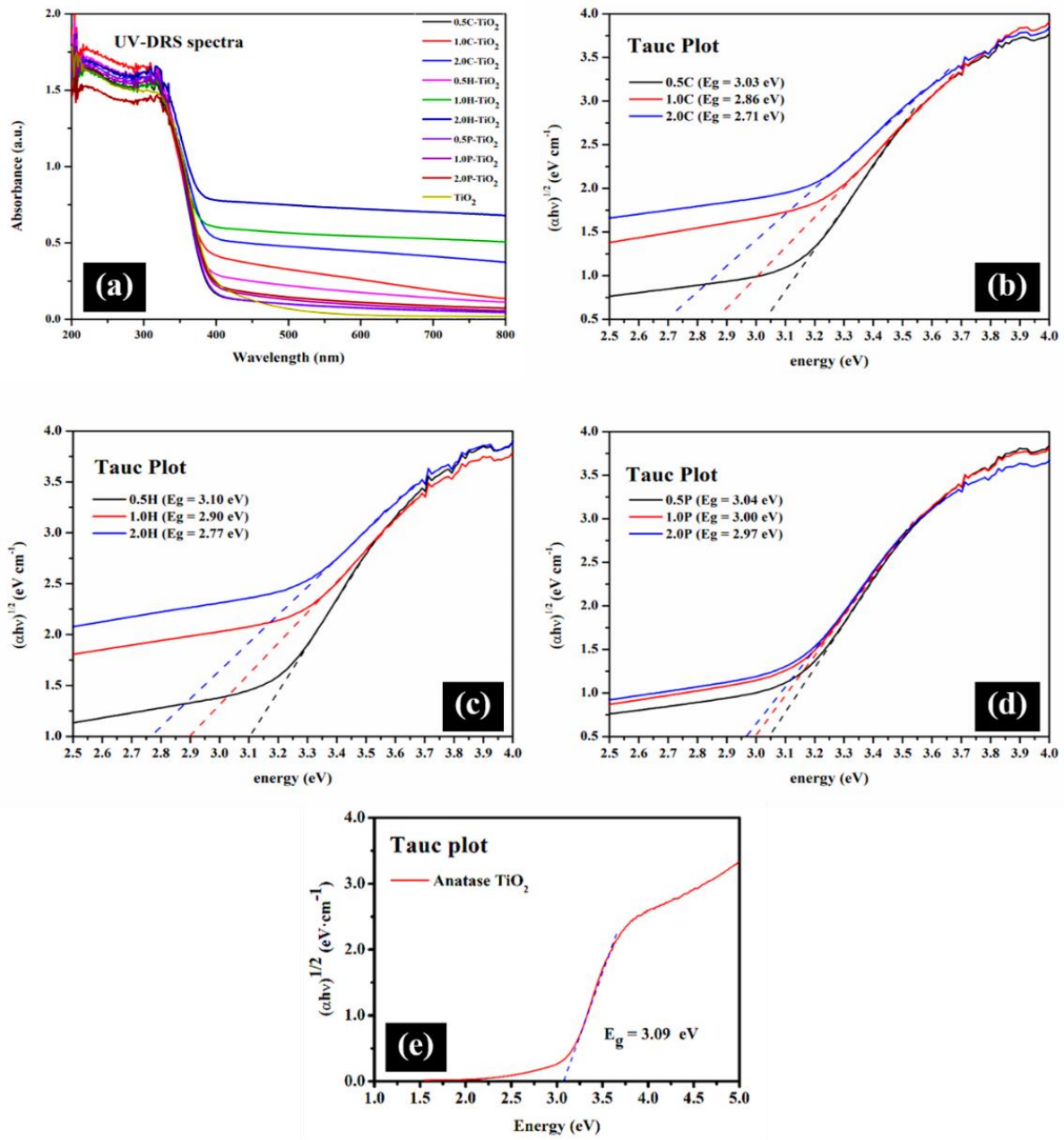


Fig. 7. (a) The UV– DRS spectra of all synthesized C–doped anatase TiO₂ and Tauc plot spectra of C–doped anatase TiO₂ which carbon sources from (b) corn starch, (c) honey, (d) PEG1500 and (e) TiO₂.

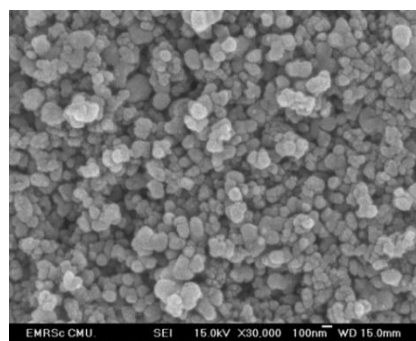


Fig. 8. The SEM image of TiO₂.

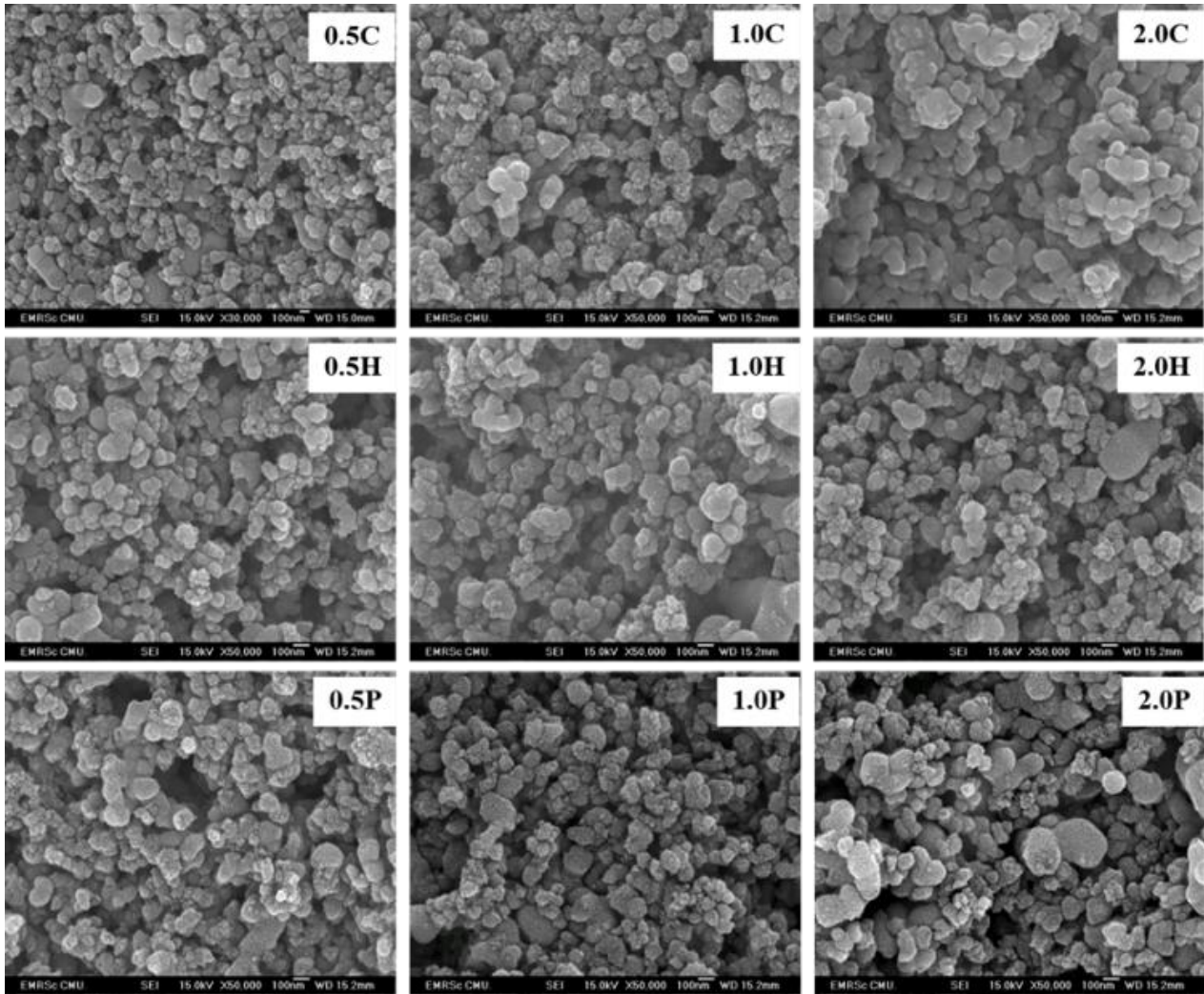


Fig. 9. SEM images of all as-synthesized C-doped TiO_2 .

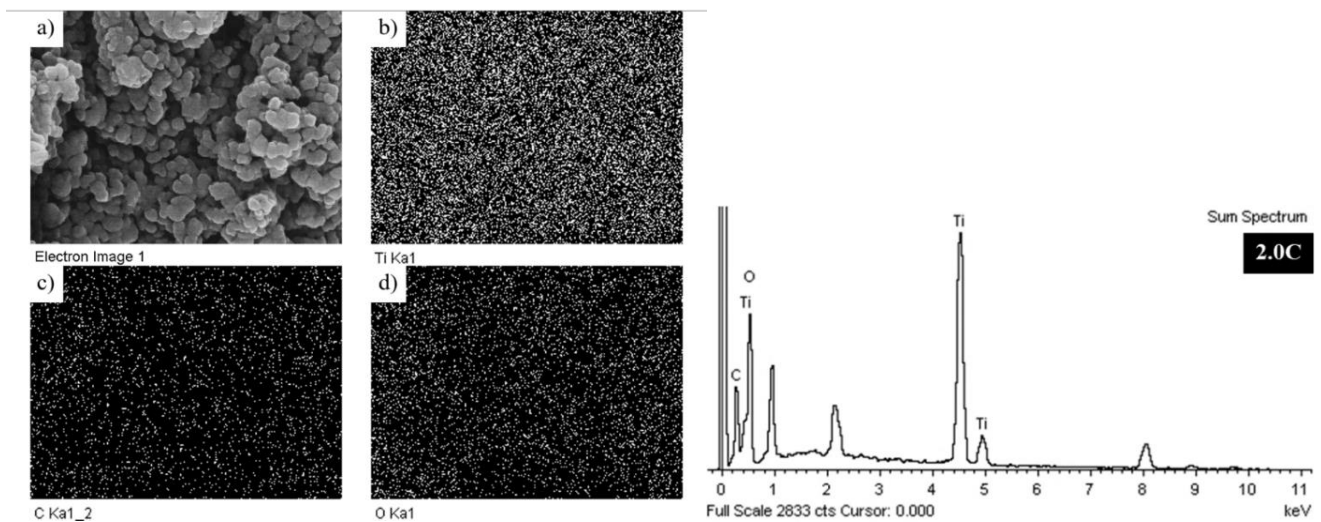


Fig. 10. (a) SEM image of the as-synthesized 2.0C- TiO_2 with 2.0%wt. carbon from corn starch and EDS mappings of (b) Ti, (c) C and (d) O elements, and (e) EDS spectrum.

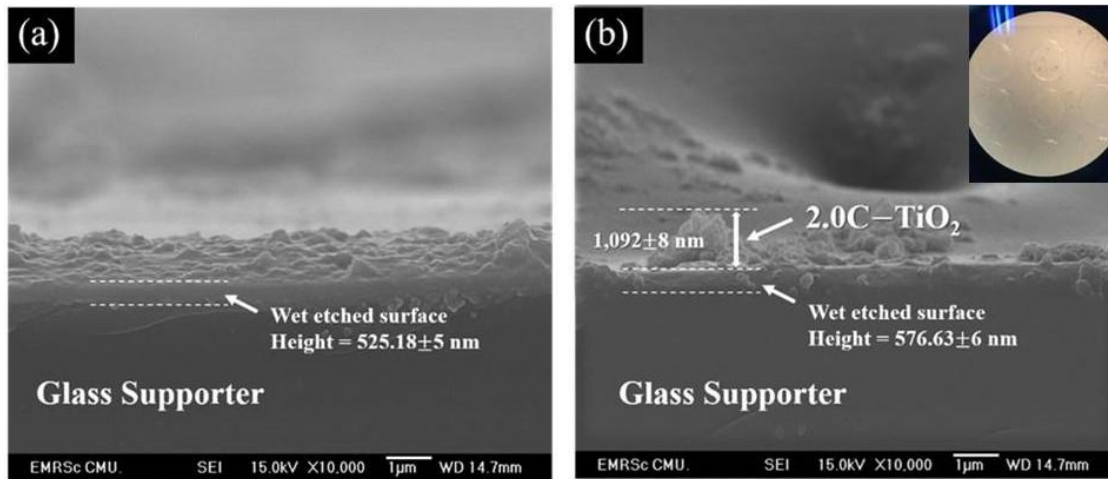


Fig. 11. Cross-section SEM images of (a) bare modified glass and (b) the as-synthesized 2.0C-TiO₂ films with top-view optical image.

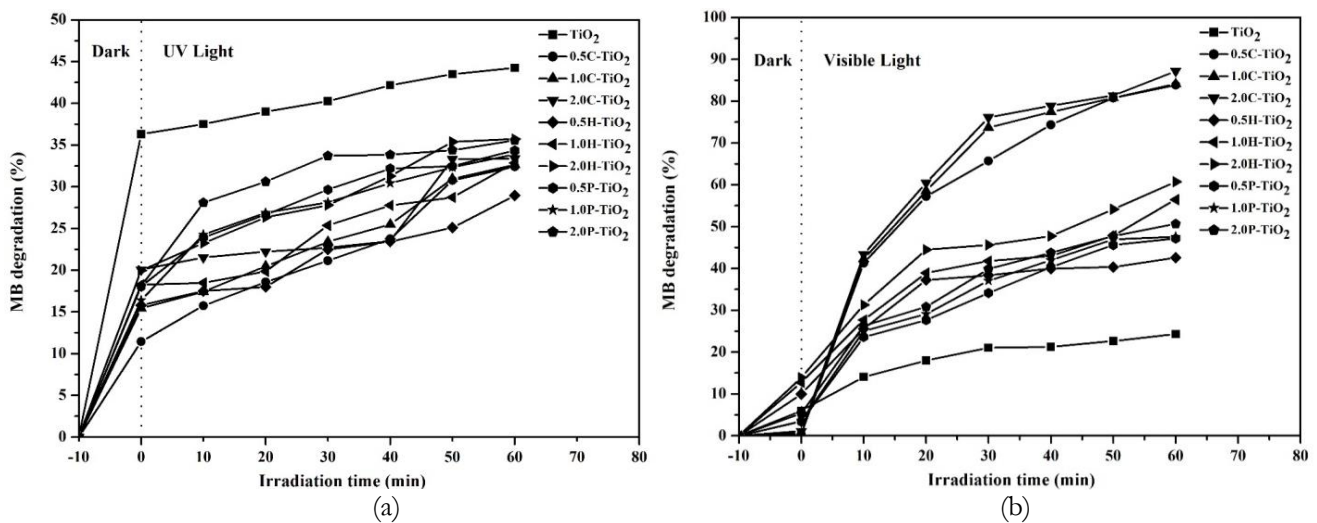


Fig. 12. MB degradation at pH 7 by using TiO₂ and all as-synthesized C-doped TiO₂ photocatalysts under (a) UV-light and (b) Vis-light.

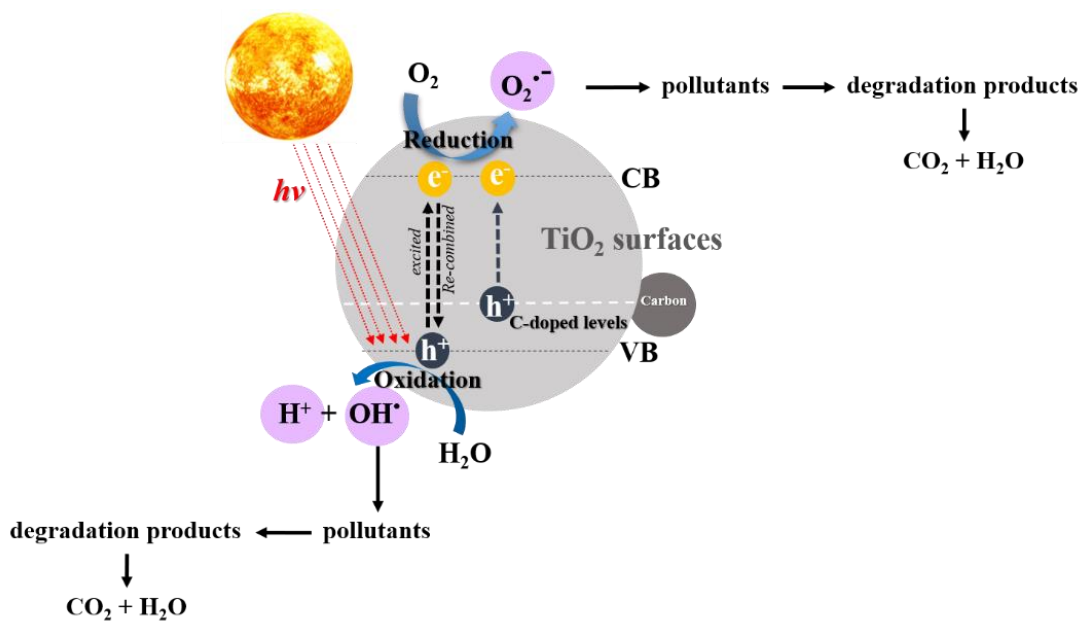
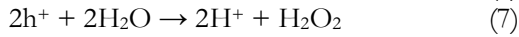


Fig. 13. Photocatalytic mechanism of C-doped TiO₂ under UV-Vis light.

After that, positive holes (h^+) at valence band and the photo-excited electrons at conduction band continue to promote the oxidative and reductive reaction. Oxidative reactions due to photocatalytic effect of positive holes at valence band as followed Eq. (6–8):



Reductive reactions due to photocatalytic effect of the photo-excited electrons at conduction band as followed (Eq. (9)–(11)):

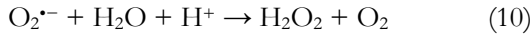


Figure 14 represents the hydroxyl radicals are generated in both types of redox reactions. These hydroxyl radicals are very oxidative and firstly attacked to MB resulted to the conjugate structure of N–S heterocyclic compound was broken and aromatic ring was oxidized to open the ring, the dye molecules were degraded and formed micro-molecular organics during photocatalysis reaction to final completely nontoxic compounds of H_2O and CO_2 as reported by X. Wang et al. (2018) [75] and R. S. Dariani and coworkers (2016) [76].

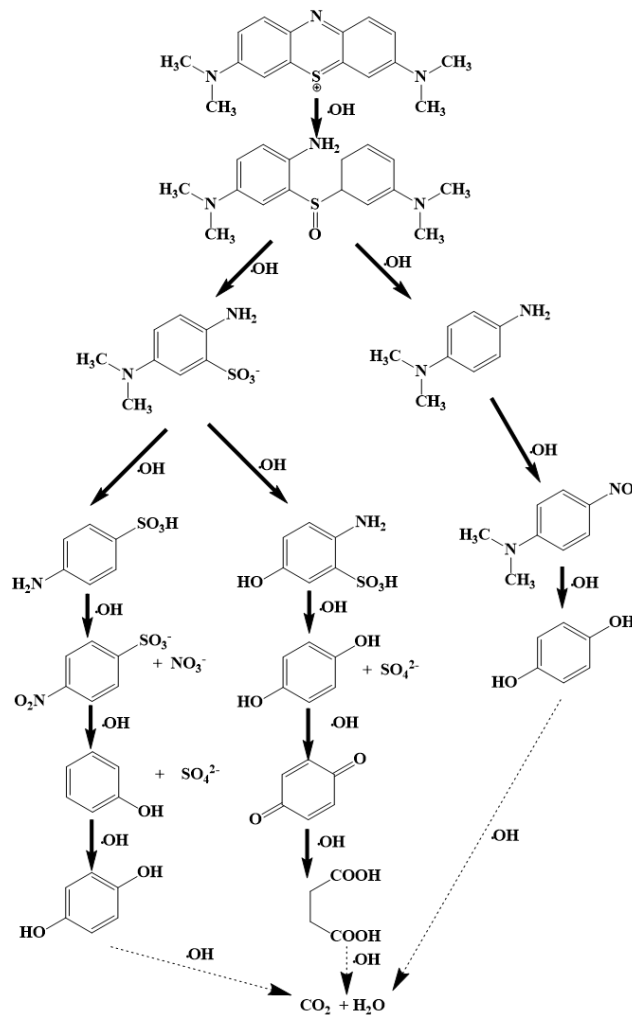


Fig. 14. The photocatalytic oxidation degradation of MB.

4. Conclusion

In this study, successfully optimized the 2%wt. carbon doping on the C-doped anatase TiO_2 nanoparticles were synthesized by ultrasonic assisted sol-gel method. The external different carbon sources affected clearly on the optical and photocatalytic properties of anatase TiO_2 . UV-DRS spectra showed the narrowed band gap of TiO_2 when maximal doped with 2%wt carbon source from corn starch for the enhancing

Vis-light photocatalysis response which agreement with the high photocatalytic efficiency of 87% MB removal or 4 times higher than TiO_2 . Moreover, the synthesis of C-doped anatase TiO_2 via ultrasonic assisted sol-gel method can be produced the photocatalyst in nanoscale with more surface area, in addition to, utilized the modified glass slide as supported for degrading the organic pollutant under the Vis-light processes. Finally, this can be demonstrated for large scale application with low cost of purification of wastewater industry.

Acknowledgement

The authors were grateful to thank for financial support obtained from Center of Excellence for Innovation in Chemistry (PERCH-CIC) for financial support.

References

- [1] K. Nakata and A. Fujishima, "TiO₂ photocatalysis: design and applications," *J. Photochem. Photobiol., C*, vol. 13, no. 3, pp. 169–189, 2012.
- [2] J. M. Coronado, F. Fresno, M. D. Hernández-Alonso, and R. Portela, "A historical introduction to photocatalysis," *Design of Advanced Photocatalytic Materials for Energy and Environmental Applications*, pp. 1–4, 2013.
- [3] P. S. Basavarajappa, S. B. Patil, N. Ganganagappa, K. R. Reddy, A. V. Raghu, and C. V. Reddy, "Recent progress in metal-doped TiO₂, non-metal doped/codoped TiO₂ and TiO₂ nanostructured hybrids for enhanced photocatalysis," *Int. J. Hydrogen Energy*, vol. 45, no. 13, pp. 7764–7778, 2020.
- [4] P. Hajkova, P. Spatenka, J. Horsky, I. Horska, and A. Kolouch, "A. Photocatalytic effect of TiO₂ films on viruses and bacteria," *Plasma Process Polym.*, vol. 4, no. 1, pp. S397-S401, 2007.
- [5] N. Miranda-García, M. I. Maldonado, J. M. Coronado, and S. Malato, "Degradation study of 15 emerging contaminants at low concentration by immobilized TiO₂ in a pilot plant," *Catal. Today*, vol. 151, no. 1-2, pp. 107-113, 2010.
- [6] O. L. Eng, Y. Choo, L. Hwei, H. C. Ong, Abd. Hamid, S. Bee, and J. C. Juan, "Recent advances of titanium dioxide (TiO₂) for green organic synthesis," *RSC Adv.*, vol. 6, pp. 108741–108754, 2016.
- [7] A. Di Paola, M. Bellardita, and L. Palmisano, "Brookite, the least known TiO₂ photocatalyst," *Catalysts*, vol. 3, pp. 36–73, 2013.
- [8] L. G. Devi and R. Kavitha, "Review on modified N–TiO₂ for green energy applications under UV/visible light: Selected results and reaction mechanisms," *RSC Adv.*, vol. 4, no. 54, pp. 28265–28299, 2014.
- [9] M. A. Henderson, "A surface science perspective on TiO photocatalysis," *Surf. Sci. Rep.*, vol. 66, pp. 185-297, 2011.
- [10] M. Khairy and W. Zakaria, "Effect of metal-doping of TiO₂ nanoparticles on their photocatalytic activities toward removal of organic dyes," *Egypt. J. Pet.*, vol. 23, no. 4, pp. 419-426, 2014.
- [11] S. Manu and M. Abdul Khadar, "Non-uniform distribution of dopant iron ions in TiO₂ nanocrystals probed by X-ray diffraction, Raman scattering, photoluminescence and photocatalysis," *J. Mater. Chem. C.*, Vol. 3, pp. 1846-1853, 2015.
- [12] C. Diaz-Urbe, W. Vallejo, and W. Ramos, "Methylene blue photocatalytic mineralization under visible irradiation on TiO₂ thin films doped with chromium," *Appl. Surf. Sci.*, vol. 319, no. 15, pp. 121–127, 2014.
- [13] S. Wang, X. Zhang, D. Ma, Z. Yu, X. Wang, and Y. Niu, "Photocatalysis performance of Nb doped TiO₂ film in situ growth prepared by a micro plasma method," *Rare Metal Mat. Eng.*, vol. 43, no. 7, pp. 1549–1552, 2014.
- [14] S. Liu, E. Guo, and L. Yin, "Tailored visible-light driven anatase TiO₂ photocatalysts based on controllable metal ion doping and ordered mesoporous structure," *J. Mater. Chem.*, vol. 22, pp. 5031–5041, 2012.
- [15] E. O. Oseghe, P. G. Ndungu, and S. B. Jonnalagadda, "Photocatalytic degradation of 4-chloro-2-methylphenoxyacetic acid using W-doped TiO₂," *J. Photochem. Photobiol., A*, vol. 312, pp. 96–106, 2015.
- [16] W. Sangkhun, L. Laokiat, V. Tanboonchuy, P. Khamdahsag, and N. Grisdanurak, "Photocatalytic degradation of BTEX using W-doped TiO₂ immobilized on fiberglass cloth under visible light," *Superlattice. Microst.*, vol. 52, no. 4, pp. 632-642, 2012.
- [17] A. Mayoufi, M. F. Nsib, and A. Houas, "Doping level effect on visible-light irradiation W doped TiO₂-anatase photocatalysts for Congo red photodegradation," *C R Chim.*, vol. 17, no. 7–8, pp. 818–823, 2014.
- [18] F. Zhang, Z. Cheng, L. Kang, L. Cui, W. Liu, X. Xu, G. Hou, and H. Yang, "A novel preparation of Ag-doped TiO₂ nanofibers with enhanced stability of photocatalytic activity," *RSC Adv.*, vol. 5, pp. 32088–32091, 2015.
- [19] L. M. Santos, W. A. Machado, M. D. França, K. A. Borges, R. M. Paniago, A. O. T. Patrocínio, and A. E. H. Machado, "Structural characterization of Ag-doped TiO₂ with enhanced photocatalytic activity," *RSC Adv.*, vol. 5, pp. 103752-103759, 2015.
- [20] A. M. A. Abdel-Wahab, O. S. Mohamed, S. A. Ahmed, and M. F. Mostafa, "Ag-doped TiO₂ enhanced photocatalytic oxidation of 1,2-cyclohexanediol," *J. Phys. Org. Chem.*, vol. 25, pp. 1418–1421, 2012.
- [21] C. Zhao, X. Shu, D. C. Zhu, S. H. Wei, Y. X. Wang, M. J. Tu, and W. Gao, "High visible light photocatalytic property of Co²⁺-doped TiO₂ nanoparticles with mixed phases," *Superlattice. Microst.*, vol. 88, pp. 32–42, 2015.
- [22] I. Ganesh, A. K. Gupta, P. P. Kumar, P. S. C. Sekhar, K. Radha, G. Padmanabham, and G. Sundararajan, "Preparation and characterization of Co-doped TiO₂ materials for solar light induced

- current and photocatalytic applications,” *Mater. Chem. Phys.*, vol. 35, no. 1, pp. 220–234, 2012.
- [23] S. M. Bawaked, S. Sathasivam, D. S. Bhachu, N. Chadwick, A. Y. Obaid, S. Al-Thabaiti, S. N. Basahel, C. J. Carmalt, and I. P. Parkin, “Aerosol assisted chemical vapor deposition of conductive and photocatalytically active tantalum doped titanium dioxide films,” *J. Mater. Chem. A*, vol. 2, pp. 12849–12856, 2014.
- [24] L. R. Sheppard, J. Holik, R. Liu, S. Macartney, and R. Wuhrer, “Tantalum enrichment in tantalum-doped titanium dioxide,” *J. Am. Ceram. Soc.*, vol. 97, no. 12, pp. 3793–3799, 2014.
- [25] J. Majeed, C. Nayak, S. N. Jha, K. Bhattacharyya, D. Bhattacharyy, and A. K. Tripathi, “Correlation of Mo dopant and photocatalytic properties of Mo incorporated TiO₂: An EXAFS and photocatalytic study,” *RSC Adv.*, vol. 5, pp. 90932–90940, 2015.
- [26] J. Li, D. Wang, H. Liu and Z. Zhu, “Multilayered Mo-doped TiO₂ nanofibers and enhanced photocatalytic activity,” *Mater. Manuf. Process.*, vol. 27, no. 6, pp. 631–635, 2012.
- [27] S. Wang, L. N. Bai, H. M. Sun, Q. Jiang, and J. S. Lian, “Structure and photocatalytic property of Mo-doped TiO₂ nanoparticles,” *Powder Technol.*, vol. 244, pp. 9–15, 2013.
- [28] V. D. Binasa, K. Sambani, T. Maggosc, A. Katsanaki, and G. Kiriakidis, “Synthesis and photocatalytic activity of Mn-doped TiO₂ nanostructured powders under UV and visible light,” *Appl. Catal. B*, vol. 113–114, pp. 79–86, 2012.
- [29] M. E. Olya, A. Pirkarami, M. Soleimani, and M. Bahmaei, “Photoelectrocatalytic degradation of acid dye using Ni-TiO₂ with the energy supplied by solar cell: Mechanism and economical studies,” *J. Environ. Econ. Manage.*, vol. 121, pp. 210–219, 2013.
- [30] C. Y. Chen, and L. J. Hsu, “Kinetic study of self-assembly of Ni(II)-doped TiO₂ nanocatalysts for the photodegradation of azo pollutants,” *RSC Adv.*, vol. 5, pp. 88266–88271, 2015.
- [31] R. Vasilic, S. Stojadinovic, N. Radić, P. Stefanov, Z. Dohčević-Mitrović, and B. Grbić, “One-step preparation and photocatalytic performance of vanadium doped TiO₂ coatings. *Mater. Chem. Phys.*, vol. 151, pp. 337–344, 2015.
- [32] M. Khan, Y. Song, N. Chen, and W. Cao, “Effect of V doping concentration on the electronic structure, optical and photocatalytic properties of nano-sized V-doped anatase TiO₂,” *Mater. Chem. Phys.*, vol. 142, no. 1, pp. 148–153, 2013.
- [33] P. Pongwan, B. Inceesungvorn, K. Wetchakun, S. Phanichphant, and N. Wetchakun, “Highly efficient visible-light-induced photocatalytic activity of Fe-doped TiO₂ nanoparticles,” *Eng. J.*, vol. 16, no. 3, pp. 143–151, 2012.
- [34] J. Xu, Y. Ao, M. Chen, and D. Fu, “Photoelectrochemical property and photocatalytic activity of N-doped TiO₂ nanotube arrays,” *Appl. Surf. Sci.*, vol. 256, no. 13, pp. 4397–4401, 2010.
- [35] S.-J. Ha, D. H. Kim, and J. H. Moon, “N-doped mesoporous inverse opal structures for visible-light photocatalysts,” *RSC. Adv.*, vol. 5, no. 95, pp. 77716–77722, 2015.
- [36] A. V. Emeline, V. N. Kuznetsov, V. K. Rybchuk, and N. Serpone, “Visible-light-active titania photocatalysts: the case of N-doped TiO₂s—Properties and some fundamental issues,” *Int. J. Photoenergy*, vol. 2008. ID: 258394.
- [37] M. Wang, J. Han, Y. Hu, and R. Guo, “Mesoporous C, N-codoped TiO₂ hybrid shells with enhanced visible light photocatalytic performance,” *RSC. Adv.*, vol. 7, pp. 15513–15520, 2017.
- [38] J. Yu, G. Dai, Q. Xiang, and M. Jaroniec, “Fabrication and enhanced visible-light photocatalytic activity of carbon self-doped TiO₂ sheets with exposed {001} facets,” *J. Mater. Chem.*, vol. 21, pp. 1049–1057, 2011.
- [39] N. A. Sean, W. L. Leaw, and H. Nur, “Effect of calcination temperature on the photocatalytic activity of carbon-doped titanium dioxide revealed by photoluminescence study,” *J. Chin. Chem. Soc.-Taip.*, vol. 66, no. 10, pp. 1277–1283, 2019.
- [40] V. Štengl, V. Houšková, S. Bakardjieva, and N. Murafa, “Photocatalytic activity of boron modified titania under UV and visible-light illumination,” *ACS Appl. Mater. Interfaces.*, vol. 2, no. 2, pp. 575–580, 2010.
- [41] X. Wang, M. Blackford, K. Prince, and R. A. Caruso, “Preparation of boron-doped porous titania networks containing gold nanoparticles with enhanced visible-light photocatalytic activity,” *ACS Appl. Mater. Interfaces.*, vol. 4, no. 1, pp. 476–482, 2012.
- [42] N. Patel, A. Dashora, R. Jaiswal, R. Fernandes, M. Yadav, D. C. Kothari, B. L. Ahuja, and A. Miotello, “Experimental and theoretical investigations on the activity and stability of substitutional and interstitial boron in TiO₂ photocatalyst,” *J. Phys. Chem. C*, vol. 119, no. 32, pp. 18581–18590, 2015.
- [43] S. A. Bakar, and C. Ribeiro, “A comparative run for visible-light driven photocatalytic activity of anionic and cationic S doped TiO₂ photocatalysts: A case study of possible sulfur doping through chemical protocol,” *J. Mol. Catal. A-Chem.*, vol. 421, pp. 1–15, 2016.
- [44] Z. Huang, Z. Gao, S. Gao, Q. Wang, Z. Wang, B. Huang, and Y. Dai, “Facile synthesis of S-doped reduced TiO_{2-x} with enhanced visible-light photocatalytic performance,” *Chinese J. Catal.*, vol. 38, no. 5, pp. 821–830, 2017.
- [45] Q. Gao, F. Si, S. Zhang, Y. Fang, X. Chen, and S. Yang, “Hydrogenated F-doped TiO₂ for photocatalytic hydrogen evolution and pollutant degradation,” *Int. J. Hydrogen Energ.*, vol. 44, no. 16, pp. 8011–8019, 2019.

- [46] A. Kafizas, N. Noor, P. Carmichael, D. O. Scanlon, C. J. Carmalt, and I. P. Parkin, "Combinatorial atmospheric pressure chemical vapor deposition of F: TiO₂: The relationship between photocatalysis and transparent conducting oxide properties," *Adv. Funct. Mater.*, vol. 24, no. 12, pp. 1758–1771, 2014.
- [47] M. V. Dozzi, C. D'Andrea, B. Ohtani, G. Valentini, and E. Selli, "Fluorine-doped TiO₂ materials: photocatalytic activity vs time-resolved photoluminescence," *J. Phys. Chem. C*, vol. 117, no. 48, pp. 25586–25595, 2013.
- [48] P. C. S. Bezerra, R. P. Cavalcante, A. Garcia, H. Wender, M. A. U. Martines, G. A. Casagrande, J. Giménez, P. Marco, S. C. Oliveira, and Jr.-A. Machulek, "Synthesis, characterization, and photocatalytic activity of pure and N-, B-, or Ag-doped TiO₂," *J. Braz. Chem. Soc.*, vol. 28, no. 9, pp. 1788–1802, 2017.
- [49] A. E. Giannakas, E. Seristatidou Y. Deligiannakis, and I. Konstantinou, "Photocatalytic activity of N-doped and N-F co-doped TiO₂ and reduction of chromium(VI) in aqueous solution: An EPR study," *Appl. Catal. B*, vol. 132–133, pp. 460–468, 2013.
- [50] G. Wu, T. Nishikawa, B. Ohtani, and A. Chen, "Synthesis and characterization of carbon-doped TiO₂ nanostructures with enhanced visible light response," *Chem. Mater.*, vol. 19, no. 18, pp. 4530–4537, 2007.
- [51] Y. Park, W. Kim, H. Park, T. Tachikawa, T. Majima, and W. Choi, "Carbon-doped TiO₂ photocatalyst synthesized without using an external carbon precursor and the visible light activity," *Appl. Catal. B*, vol. 91, no. 1–2, pp. 355–361, 2009.
- [52] S. Sakthivel, and H. Kisch, "Daylight photocatalysis by carbon-modified titanium dioxide," *Angew. Chem.*, vol. 42, pp. 4908–4911, 2003.
- [53] L. Zhao, X. Chen, X. Wang, Y. Zhang, W. Wei, Y. Sun, M. Antonietti, and M. M. Titirici, "One-step solvothermal synthesis of a carbon@TiO₂ dyade structure effectively promoting visible-light photocatalysis," *Adv. Mater.*, vol. 22, no. 30, pp. 3317–3321, 2010.
- [54] T. T. Lim, P. S. Yap, M. Srinivasan, and A. G. Fane, "TiO₂/AC composites for synergistic adsorption-photocatalysis processes: Present challenges and further developments for water treatment and reclamation," *Crit. Rev. Environ. Sci. Technol.*, vol. 41, no. 13, pp. 1173–1230, 2011.
- [55] S. Sun, R. Zhao, Y. Xie, and Y. Liu, "Photocatalytic degradation of aflatoxin B1 by activated carbon supported TiO₂ catalyst," *Food Control.*, vol. 100, pp. 183–188, 2019.
- [56] F. Dong, S. Guo, H. Wang, X. Li, and Z. Wu, "Enhancement of the visible-light photocatalytic activity of C-doped TiO₂ nanomaterials prepared by a green synthetic approach," *J. Phys. Chem. C.*, vol. 115, no. 27, pp. 13285–13292, 2011.
- [57] E. M. Neville, M. J. Mattle, D. Loughrey, B. Rajesh, M. Rahman, J.M. D. MacElroy, J. A. Sullivan, and K. R. Thampi, "Carbon-doped TiO₂ and carbon, tungsten-codoped TiO₂ through sol-gel processes in the presence of melamine borate: Reflections through photocatalysis," *J. Phys. Chem. C.*, vol. 116, no. 31, pp. 16511–16521, 2012.
- [58] T. An, J. Chen, X. Nie, G. Li, H. Zhang, X. Liu, and H. Zhao, "Synthesis of carbon nanotube-anatase TiO₂ sub-micrometer-sized sphere composite photocatalyst for synergistic degradation of gaseous styrene," *ACS Appl. Mater. Interfaces*, vol. 4, no. 11, pp. 5988–5996, 2012.
- [59] F. Venditti, F. Cuomo, A. Ceglie, P. Avino, M. V. Russo, and F. Lop, "Visible light caffeic acid degradation by carbon-doped titanium dioxide," *Langmuir*, vol. 31, no. 12, pp. 3627–3634, 2015.
- [60] J. Zhang, M. Vasei, Y. Sang, H. Liu, and J. P. Claverie, "TiO₂@carbon photocatalysts: the effect of carbon thickness on catalysis," *ACS Appl. Mater. Interfaces.*, vol. 8, no. 3, pp. 1903–1912, 2016.
- [61] M. Robotti, S. Dosta, C. Fernández-Rodríguez, M. J. Hernández-Rodríguez, I. G. Cano, E. P. Melián, and J. M. Guilemany, "Photocatalytic abatement of NO_x by C-TiO₂/polymer composite coatings obtained by low pressure cold gas spraying," *Appl. Surf. Sci.*, vol. 362, pp. 274–280, 2016.
- [62] W. I. Nawawia, A. Y. Anib, M. A. M. Ishakb, A. Ramlib, M. S. Azamib, F. Zaidb, F. Bakarib, R. Zaharudin, "Modification and characterization of C-doped TiO₂ photocatalysts for photodegradation of reactive red (RR4)," *Desalin. Water Treat.*, vol. 113, pp. 254–261, 2018.
- [63] N. R. Khalida, A. Majida, M. Bilal Tahira, N. A. Niazb, Sadia Khalidc, "A review," *Ceram. Int.*, vol. 43, Issue 17, pp. 14552–14571, 2017.
- [64] U. Diebold, "The surface science of titanium dioxide," *Surf. Sci. Rep.*, vol. 48, no. 5–8, pp. 53–229, 2003.
- [65] H.-G. Park, J. I. Kim, M. Kang and M.-K. Yeo, "The effect of metal-doped TiO₂ nanoparticles on zebrafish embryogenesis," *Mol. Cell. Toxicol.* vol. 10, pp.293–301, 2014.
- [66] M. V. Dozzi and E. Selli, "Doping TiO₂ with p-block elements: Effects on photocatalytic activity," *J. Photochem. Photobiol. C*, vol. 14, pp. 13–28, 2013.
- [67] S. Narakaew, "The nano-TiO₂ synthesis using ultrasonic assisted sol-gel method and its photocatalytic degradation of methylene blue," *J. Ceram. Process Res.*, vol. 18, no. 1, pp. 36–40, 2017.
- [68] J. Zhang, P. Zhou, J. Liu, and J. Yu, "New understanding of the difference of photocatalytic activity among anatase, rutile and brookite TiO₂," *Phys. Chem. Chem. Phys.*, vol. 16, no. 38, pp. 20382–20386, 2014.
- [69] M. M. Karkare, "The direct transition and not indirect transition, is more favourable for band gap calculation of anatase TiO₂ nanoparticles," *Int. J. Sci. Eng. Res.*, vol. 6, no. 12, pp. 48–53, 2015.
- [70] A. H. D. Abdullah1, S. Chalimah, I. Primadona and M. H. G. Hanantyo, "Physical and chemical

- properties of corn, cassava, and potato starchs,” *IOP Conf. Series: Earth and Environmental Science*, vol. 160, pp. 012003, 2018.
- [71] H. S. Chen and R. V. Kumar, “Sol–gel TiO₂ in self-organization process: Growth, ripening and sintering,” *RSC Adv.*, vol. 2, no. 6, pp. 2294–2301, 2012.
- [72] F. Sayilkan, M. Asilturk, H. Sayilkan, Y. Önal, M. Akarsu, and E. Arpaç, “Characterization of TiO₂ synthesized in alcohol by a sol-gel process: The effects of annealing temperature and acid catalyst,” *Turk. J. Chem.*, vol. 29, pp. 697–706, 2005.
- [73] S. Mahshid, M. Askari, and M. Sasani Ghamsari, “Synthesis of TiO₂ nanoparticles by hydrolysis and peptization of titanium isopropoxide solution,” *J. Mater. Process Technol.*, vol. 189, no. 1–3, pp. 296–300, 2007.
- [74] Z. A. C. Ramli, N. Asim, W. R. W. Isahak, Z. Emdadi, N. Ahmad–Ludin, M. A. Yarmo, and K. Sopian, “Photocatalytic degradation of methylene blue under UV-light irradiation on prepared carbonaceous TiO₂,” *Sci. World J.*, vol. 2014, Article ID 415136, pp. 1–8, 2014.
- [75] X. Wang, S. Han, Q. Zhang, N. Zhang, and D. Zhao, “Photocatalytic oxidation degradation mechanism study of methylene blue dye waste water with GR/iTiO₂,” *MATEC Web Conf.*, vol. 238, Article ID: 03006, 2018.
- [76] R. S. Dariani, A. Esmaceli, A. Mortezaali and S. Dehghanpour, “Photocatalytic reaction and degradation of methylene blue on TiO₂ nano-sized particles,” *Optik.*, vol. 127, no.18, pp. 7143–7154, 2016.
- [77] Q. Deng, W. Zhang, T. Lan, J. Xie, W. Xie, Z. Liu, Y. Huang and M. Wei, “Anatase TiO₂ quantum dots with a narrow band gap of 2.85 eV based on surface hydroxyl groups exhibiting significant photodegradation property,” *Eur. J. Inorg. Chem.*, vol. 2018, no. 13, pp. 1506–1510, 2018.
- [78] A. Al-Mokaram, R. Yahya, M. M. Abdi and H. Mahmud, “The development of non-enzymatic glucose biosensors based on electrochemically prepared polypyrrole-chitosan-titanium dioxide nanocomposite films,” *J. Nanomater.*, vol. 7, no. 129, pp. 1–22, 2017.
- [79] D. Li, Z. Xing, X. Yu and X. Cheng, “One-step hydrothermal synthesis of C-N-S-tridoped TiO₂-based nanosheets photoelectrode for enhanced photoelectrocatalytic performance and mechanism,” *Electrochim. Acta.*, vol. 170, pp. 182–190, 2015.
- [80] I. A. Appavoo, J. Hu, Y. Huang, S. F. Y. Li and S. L. Ong, “Response surface modeling of Carbamazepine (CBZ) removal by Graphene-P25 nanocomposites/UVA process using central composite design,” *Water. Res.*, vol. 57, pp. 270–279, 2014.
- [81] K. S. Kim, and M. A. Barteau, “Structure and composition requirements for deoxygenation, dehydration, and ketonization reactions of carboxylic acids on TiO₂(001) single-crystal surfaces,” *J. Catal.*, vol. 125, no. 2, pp. 353–375, 1990.
- [82] X. X. Zou, G. D. Li, J. Zhao, J. Su, X. Wei, K. X. Wang, Y. N. Wang and J. S. Chen, “Light-driven preparation, microstructure, and visible-light photocatalytic property of porous carbon-doped TiO₂,” *Int. J. Photoenergy.*, Article ID 720183, pp. 1–9, 2012.



Sittipong Au-pree is a graduate student at the Applied Chemistry Program, Department of Applied Chemistry, Faculty of Science, Lampang Rajabhat University. He received his B.Sc. (Chemistry) from Sakon Nakhon Rajabhat University. His research interests include photocatalysis and materials science.



Phiphop Narakaew is a lecturer at the Department of Physics, Faculty of Science, Lampang Rajabhat University. He received his B.Ed. (Physics) from Naresuan University and M.Sc. (Physics) from Silpakorn University. His research interests include materials science and alternative energy.



Siwat Thungprasert is a lecturer at the Department of Applied Chemistry, Faculty of Science, Lampang Rajabhat University. He received his B.Sc. (Chemistry), M.Sc. (Chemistry) and Ph.D. (Chemistry) from Chiang Mai University. His research interests include materials science and catalysis for fuel cells.



Theeraporn Promanan is a lecturer at the Department of Applied Chemistry, Faculty of Science, Lampang Rajabhat University. She received his B.Sc. (Chemistry), M.Sc. (Chemistry) and Ph.D. (Chemistry) from Chiang Mai University. Her research interests include materials science and alternative energy.



Aphiruk Chaisena is an associate professor at the Department of Applied Chemistry, Faculty of Science, Lampang Rajabhat University. He received his B.Ed (Chemistry) from Chiang Mai Teacher College, M.Sc. (Teaching Chemistry) from Chiang Mai University and Ph.D. (Chemistry) from Suranaree University of Technology. His research interests include materials chemistry, nanomaterials, porous materials, and electrocatalyst fuel cell.



Samroeng Narakaew is an assistant professor at the Department of Applied Chemistry, Faculty of Science, Lampang Rajabhat University. She received her B.Sc. (Chemistry) from Khon Kaen University and Ph.D. (Chemistry) from Suranaree University of Technology. Her research interests include materials science, photocatalysis, crystallography, and alternative energy.